McCue, Scott W. and King, John R. and Riley, David S. (2003) Extinction Behaviour of Contracting Bubbles in Porous Media. *Quarterly Journal of Mechanics and Applied Mathematics* 56(3):pp. 455-482.

# EXTINCTION BEHAVIOUR OF CONTRACTING BUBBLES IN POROUS MEDIA

S. W. McCue, J. R. King and D. S. Riley
Division of Theoretical Mechanics
School of Mathematical Sciences
University of Nottingham
Nottingham NG7 2RD, UK.

10 February 2003

**Abstract**

This paper is concerned with bubble contraction in porous media otherwise filled with viscous fluid. We suppose that an external pressure is applied to the (fixed) boundary of a porous medium, forcing a bubble to contract towards a point. By using the Baiocchi transform, we are able to give a rather complete asymptotic description of the process at times just before the bubble vanishes. The application of time-reversal to the results leads to implications for bubble nucleation.

## 1 Introduction

Much attention has been given to free boundary problems arising as models of fluid flow through porous media; see, for example, Elliott and Ockendon [5] or Crank [2]. Typically, these models have applications to groundwater flow and oil/gas recovery. Here the free boundary describes what is taken to be a sharp interface between two different fluids. In the case of groundwater flow the interface is usually between water and air, or fresh water and salt water, while for oil/gas recovery the interface could be between oil and water or between water and gas. In this study we are interested in the situation where there is a large viscosity contrast between the fluids so that one of the them may be considered as a simply-connected bubble of inviscid fluid. Outside the bubble the porous medium is saturated with a viscous fluid. The incompressibility of the viscous fluid together with Darcy's law combine to give Laplace's equation, the governing

equations and boundary conditions being the same as those of the classical Stefan problem in the limit of negligible specific heat. In two dimensions the governing equations also describe the evolution of a bubble in a Hele-Shaw cell when surface tension is negligible.

Aspects of the evolution of three-dimensional bubbles through infinite regions of a porous medium saturated with viscous fluid have been studied by Howison [9] and Entov and Etingof [6]. The flow is driven by inviscid fluid injected into or extracted from the bubble or, equivalently for most purposes, viscous fluid injected or extracted at infinity. Howison [9] considered expanding bubbles and constructed solutions in which the bubble is ellipsoidal. Di Benedetto and Friedman [4] go further, and prove that in $\mathbb{R}^N$ ($N \geq 2$) solutions with ellipsoidal bubble boundaries (with constant aspect ratios) are the only type to exist for all time (in the two-dimensional limit these bubble boundaries are ellipses with constant eccentricity). Entov and Etingof [6] considered bubbles which contract at a uniform rate. As with expanding bubbles, the only solutions that keep their shape while shrinking are ellipsoids (the relationship between the two cases follows from the time-reversibility of the problem). The effect of singularities in the flow field was also considered and, with the use of a Newtonian potential, a method of computing the points at which the bubbles vanish was developed.

For the case of Hele-Shaw flow, Entov and Etingof [6] also consider a variation of the above problem in which fluid is injected into a finite cell which initially contains a bubble of inviscid fluid (air, say). The injection takes place around the boundary in such a way that the pressure is held constant there, the problem being viewed as a model for the filling of moulds with molten material. Entov and Etingof [6] generalise their infinite domain approach to allow for this fixed boundary, and show how to compute the points where the bubbles vanish, as well as the time it takes for the bubble to disappear. They also show that the shape of the bubbles just before extinction is elliptic, regardless of the geometry of the fixed boundary (the mould shape). A recipe for computing the eccentricity of these ellipses was also given. In this paper we consider the three-dimensional version of this problem, whereby viscous fluid is injected into a cell containing an inviscid fluid. The injection continues until the bubble contracts to a point in space and the cell is completely filled with the viscous fluid. With the use of a Baiocchi transform, we give a detailed asymptotic analysis of the solution at times leading up to bubble extinction. Contained within this analysis is a simple method for determining the time and location at which the bubble vanishes, together with its asymptotic form. These

results represent a natural extension to those for the two-dimensional case.

The paper can be summarised as follows. In section 2 we formulate the problem mathematically and explain how the governing equations also describe the classical Stefan problem with infinite Stefan number. Section 3 contains all the analysis, although some of the details are relegated to appendix A. In section 4 we illustrate the extinction behaviour by presenting two examples with simple geometry. Finally, the paper closes in section 5 with discussion.

# 2 Formulation

Consider a finite region $B \subset \mathbb{R}^3$ of porous medium which is saturated with an inviscid gas. Suppose an incompressible, viscous fluid is injected into the boundary of $B$ (denoted by $\partial B$) so that the pressure $u$ is constant there. As a result, the bubble of gas will occupy a contracting region $\Omega(t)$ of the porous medium ($\Omega(t) \subseteq B$). We denote the free boundary between the two fluids by $\partial\Omega$ given by $t = \omega(x, y, z)$, where $t$ is time and $(x, y, z)$ are Cartesian coordinates. For an incompressible viscous fluid governed by Darcy's law we have

$$\boldsymbol{\nabla} \cdot \mathbf{v} = 0, \quad \mathbf{v} = -\frac{k}{\mu}\nabla p \quad \text{in} \quad B \setminus \Omega(t),$$

where $\mathbf{v}$ is the fluid velocity, $p$ the pressure, $k$ the permeability and $\mu$ the viscosity. Inside the bubble the pressure is taken to be a function of time only, the viscosity being negligible. Thus we have

$$\nabla^2 p = 0 \quad \text{in} \quad B \setminus \Omega(t), \tag{1}$$

$$p = P_E(t) \quad \text{on} \quad \partial B, \tag{2}$$

$$p = P_B(t), \quad V_n = -\frac{k}{\mu}\frac{\partial p}{\partial n} \quad \text{on} \quad \partial\Omega, \tag{3}$$

where $P_E(t)$ is the externally imposed pressure, $P_B(t)$ is the bubble pressure, and $\partial/\partial n$ is the normal derivative and $V_n$ the normal velocity of the moving boundary, directed into $\Omega(t)$. Hence $P_E$ is specified and $P_B$ can be simply expressed in terms of the volume of $\Omega$ under adiabatic or isothermal conditions; as we now show, the evolution of $P_B$ can be decoupled from the rest of the problem by introducing a suitable time variable. Specifically, we introduce the non-dimensionalisation

$$u = \frac{(p - P_B)}{P_E - P_B}, \quad \hat{\mathbf{x}} = \frac{\mathbf{x}}{l}, \quad \hat{t} = \frac{k}{\mu l^2}\int_0^t (P_E(t') - P_B(t'))dt', \quad \hat{V}_n = \frac{\mu l V_n}{k(P_E - P_B)},$$

where $l$ is a representative lengthscale of $B$. After dropping the hats we then have (for $P_E > P_B$)

$$\frac{\partial^2 u}{\partial x^2} + \frac{\partial^2 u}{\partial y^2} + \frac{\partial^2 u}{\partial z^2} = 0 \quad \text{in} \quad B \setminus \Omega(t), \tag{4}$$

with

$$u = 1 \quad \text{on} \quad \partial B \tag{5}$$

and

$$u = 0, \quad V_n = -\frac{\partial u}{\partial n} \quad \text{on} \quad t = \omega(x, y, z). \tag{6}$$

For our purposes it proves convenient to rewrite the last condition in the form

$$\boldsymbol{\nabla} u \cdot \boldsymbol{\nabla} \omega = -1 \quad \text{on} \quad t = \omega(x, y, z). \tag{7}$$

The boundary-value problem (4)-(7) can also be interpreted as a Stefan problem. Consider a finite region of fluid $B$ which is initially at its fusion temperature. If the temperature of the boundary of the fluid $\partial B$ is suddenly dropped then the fluid will solidify inwards. Here the free boundary, denoted by $\tilde{t} = \tilde{\omega}(x, y, z)$ where $\tilde{t}$ is time, divides the solid and liquid phases. Suppose that heat transport takes place through conduction only, and that there is no change of density on solidification. Then after suitable scalings (see King, Riley & Wallman [11]) we find the problem reduces to solving the heat equation

$$\frac{\partial \tilde{u}}{\partial \tilde{t}} = \frac{\partial^2 \tilde{u}}{\partial x^2} + \frac{\partial^2 \tilde{u}}{\partial y^2} + \frac{\partial^2 \tilde{u}}{\partial z^2}$$

subject to $\tilde{u} = -1$ on $\partial B$, and $\tilde{u} = 0$, $\beta = \boldsymbol{\nabla} \tilde{u} \cdot \boldsymbol{\nabla} \tilde{\omega}$ on $\tilde{t} = \tilde{\omega}(x, y, z)$. Here $\beta$ is the Stefan number, which is a ratio of latent to sensible heats. For $\beta \gg 1$ we rescale time according to $\tilde{t} = \beta t$ and write $\tilde{u} \sim -u(x, y, z, t)$, $\tilde{\omega} \sim \beta \omega(x, y, z)$ as $\beta \to \infty$ to give (4)-(7) as the leading-order problem.

# 3 'Near extinction' analysis

## 3.1 Formulation

While a closed-form solution to the problem (4)-(7) can be found when $B$ is spherical (see (54)), in general the nonlinearity of the free boundary problem prevents an exact analytical approach. Somewhat surprisingly, we can nevertheless describe the behaviour of the solution

at times approaching extinction, essentially regardless of the initial geometry. The analysis for this is presented here.

First the problem is reformulated with the use of a Baiocchi transform, defined by

$$w(x,y,z,t) = \int_{\omega}^{t} u(x,y,z,t')\,dt'.$$

The resulting boundary-value problem for $w$ is given by

$$\frac{\partial^2 w}{\partial x^2} + \frac{\partial^2 w}{\partial y^2} + \frac{\partial^2 w}{\partial z^2} = 1 \quad \text{in} \quad B \setminus \Omega(t), \tag{8}$$

with

$$w = t \quad \text{on} \quad \partial B, \quad w = \frac{\partial w}{\partial n} = 0 \quad \text{on} \quad t = \omega(x,y,z). \tag{9}$$

The formulation (8)-(9) has the advantage that time appears only as a parameter, and we can therefore solve for $w$ (and the free boundary) at any time (in particular, at or near the bubble extinction time) without knowledge of the solution at previous times.

We denote the extinction time by $t_e$, the function $w$ at extinction by $w_e(x,y,z)$, and the point of extinction by $(x_e, y_e, z_e)$. We can compute $w_e$ by writing $w_e = W + t_e$ and solving the (linear) boundary-value problem

$$\frac{\partial^2 W}{\partial x^2} + \frac{\partial^2 W}{\partial y^2} + \frac{\partial^2 W}{\partial z^2} = 1 \quad \text{in} \quad B \quad \text{with} \quad W = 0 \quad \text{on} \quad \partial B, \tag{10}$$

with the point $(x_e, y_e, z_e)$ then found as the global minimum of $W$ (for simplicity we assume the domain $B$ is convex and that there is only one extinction point), so that

$$\frac{\partial W}{\partial x} = \frac{\partial W}{\partial y} = \frac{\partial W}{\partial z} = 0 \quad \text{at} \quad (x,y,z) = (x_e, y_e, z_e), \tag{11}$$

and $t_e$ is evaluated via $t_e = -W(x_e, y_e, z_e)$. The conditions (9) are then satisfied by $w_e$.

In practice this solution process is only possible analytically if the domain $B$ is such that the linear problem (10) can be solved explicitly and some simple examples are discussed in section 4. However, for the purpose of this section the only information needed is the values of the constants $a$ and $b$ in the asymptotic expression

$$w_e(x,y,z) \sim a\bar{x}^2 + b\bar{y}^2 + (\tfrac{1}{2} - a - b)\bar{z}^2 \quad \text{as} \quad (x,y,z) \to (x_e, y_e, z_e)$$

and the elements of the rotation matrix introduced below; these depend on the geometry $\partial B$, and can be determined from (10)-(11), numerically if necessary. Here $(\bar{x}, \bar{y}, \bar{z})$ are Cartesian

coordinates formed by a translation and rotation from $(x, y, z)$, namely

$$\begin{pmatrix} \bar{x} \\ \bar{y} \\ \bar{z} \end{pmatrix} = \begin{pmatrix} \cos(\theta_{\bar{x}x}) & \cos(\theta_{\bar{x}y}) & \cos(\theta_{\bar{x}z}) \\ \cos(\theta_{\bar{y}x}) & \cos(\theta_{\bar{y}y}) & \cos(\theta_{\bar{y}z}) \\ \cos(\theta_{\bar{z}x}) & \cos(\theta_{\bar{z}y}) & \cos(\theta_{\bar{z}z}) \end{pmatrix} \begin{pmatrix} x - x_e \\ y - y_e \\ z - z_e \end{pmatrix}, \tag{12}$$

where $\theta_{\bar{x}x}$ is the angle between the positive $\bar{x}$ and $x$ axes, $\theta_{\bar{x}y}$ the angle between the positive $\bar{x}$ and $y$ axes, and so on. Without any loss of generality, we may thus set $x_e$, $y_e$ and $z_e$ to be zero, so that the point of extinction coincides with the origin, and set the matrix of direction cosines in (12) to be the unit matrix, so that we have

$$w_e(x, y, z) \sim ax^2 + by^2 + (\tfrac{1}{2} - a - b)z^2 \quad \text{as} \quad (x, y, z) \to (0, 0, 0) \tag{13}$$

with $a, b > 0$, $a + b < 1/2$, $\frac{1}{4}(1 - 2a) < b < a$, so the coefficients of the $x^2$, $y^2$ and $z^2$ terms in (13) are of decreasing size.

We note here that in two dimensions the function $w_e(x, y)$ is the same as to the modified potential $\hat{\Pi}_B(x, y)$ used by Entov and Etingof [6] when they considered bubble contraction in a finite Hele-Shaw cell.

## 3.2 Asymptotic analysis

In the limit $t \to t_e^-$, the behaviour of $w$ can be analysed in two spatial regions. For the outer region, where $r = O(1)$, we have

$$w \sim w_e(x, y, z) - (t_e - t) + \tau(t_e - t)\Lambda(x, y, z) \quad \text{as} \quad t \to t_e^-. \tag{14}$$

An asymptotic expression for the function $\tau$, which tends to zero more rapidly than linearly as $t \to t_e^-$, and the prescription for the harmonic function $\Lambda$, which vanishes on the boundary $\partial B$, will be determined by matching after describing the inner solution.

The inner region corresponds to $r = O(T(t_e - t))$, where we chose to define the function $T$ so that the volume of the bubble is $4\pi T^3/3$; clearly $T \to 0$ as $t \to t_e^-$. We assume the self-similar form

$$w \sim T^2 \Phi(X, Y, Z) \quad \text{as} \quad T \to 0, \tag{15}$$

where $X = x/T$, $Y = y/T$ and $Z = y/T$. If we denote the bubble in $(X, Y, Z)$ space by $\Omega_0$, then $\Omega_0$ has volume $4\pi/3$ and the function $\Phi$ satisfies the boundary-value problem

$$\frac{\partial^2 \Phi}{\partial X^2} + \frac{\partial^2 \Phi}{\partial Y^2} + \frac{\partial^2 \Phi}{\partial Z^2} = 1 \quad \text{outside} \quad \Omega_0 \tag{16}$$

with

$$\Phi = \frac{\partial \Phi}{\partial N} = 0 \quad \text{on} \quad \partial\Omega_0 \tag{17}$$

and, in order to match with (13),

$$\Phi \sim aX^2 + bY^2 + (\tfrac{1}{2} - a - b)Z^2 - d + \frac{\kappa}{R} + O(R^{-3}) \quad \text{as} \quad R \to \infty, \tag{18}$$

where $R^2 = X^2 + Y^2 + Z^2$ and $\partial/\partial N$ is used to denote the rescaled normal derivative. The location of the free boundary, as well as the constant $d$ and the $O(R^{-3})$ terms in (18), are found as part of the solution process, which we describe in section 3.3. The coefficient $\kappa$ in (18) is determined by the definition of the function $T$. Let $D$ be a sphere with radius $R_1$ which encloses $\Omega_0$, then the divergence theorem gives

$$\int_{D\setminus\Omega_0} \left( \frac{\partial^2 \Phi}{\partial X^2} + \frac{\partial^2 \Phi}{\partial Y^2} + \frac{\partial^2 \Phi}{\partial Z^2} \right) dV = \oint_{\partial D} \frac{\partial \Phi}{\partial N}\, dS \sim \frac{4\pi}{3} R_1^2 - 4\pi\kappa + O(R^{-2}) \tag{19}$$

as $R_1 \to \infty$. But by (16) the left-hand side of (19) is also $\int_D dV - 4\pi/3$, so by taking the limit $R_1 \to \infty$ we find $\kappa = 1/3$.

It follows from (15) that the pressure $u$ in the inner region is given by

$$u = \frac{\partial w}{\partial t} \sim T \frac{dT}{dt} \Psi(X, Y, Z) \quad \text{as} \quad T \to 0, \tag{20}$$

where

$$\Psi = 2\Phi - \mathbf{X} \cdot \boldsymbol{\nabla} \Phi. \tag{21}$$

We compute $\Psi$ after solving for $\Phi$ later in this section.

To match with the outer region, we note that (18) yields as a matching condition on the outer region that

$$w \sim ax^2 + by^2 + (\tfrac{1}{2} - a - b)z^2 - dT^2 + \frac{1}{3r} T^3 + O(T^5) \quad \text{as} \quad x, y, z, T \to 0, \tag{22}$$

where $r^2 = x^2 + y^2 + z^2$. Comparing (22) with (14), we see that we should set $\tau = T^3$, so $\Lambda \sim 1/3r$ as $r \to 0$ and hence

$$\Lambda(x, y, z) = \frac{4\pi}{3} G(x, y, z),$$

where the Green's function $G$ is given by

$$\frac{\partial^2 G}{\partial x^2} + \frac{\partial^2 G}{\partial y^2} + \frac{\partial^2 G}{\partial z^2} = -\delta(x)\delta(y)\delta(z) \quad \text{in} \quad B \quad \text{with} \quad G = 0 \quad \text{on} \quad \partial B\,. \tag{23}$$

We note that

$$G \sim \frac{1}{4\pi}\left(\frac{1}{r} - K\right) \quad \text{as} \quad r \to 0,$$

for some positive (since $G - 1/4\pi r$ is harmonic in $B$ and negative on $\partial B$) constant $K$ which depends on the geometry $\partial B$, being determined as part of the solution to (23), and hence, again by comparison of (22) with (14), we find

$$t = t_e - dT^2 + \tfrac{1}{3}KT^3 + O(T^5) \quad \text{as} \quad T \to 0. \tag{24}$$

This expression can be easily inverted to give

$$T = \frac{1}{\sqrt{d}}(t_e - t)^{1/2} + \frac{K}{6d^2}(t_e - t) + O((t_e - t)^{3/2}) \quad \text{as} \quad t \to t_e^-. \tag{25}$$

The constant $d$ still remains to be determined and this requires solution of the inner problem; see (41) below.

### 3.3 Solution to inner problem

It remains to solve the inner boundary-value problem (16)-(18). From results concerning related problems on infinite domains (cf. Howison [9], Friedman and Saki [7] and Entov and Etingof [6]), it follows that $\Omega_0$ is an ellipsoid. It is thus appropriate to use ellipsoidal coordinates $(\lambda, \mu, \nu)$, defined by

$$X = \left[\frac{(\lambda^2 - p^2)(p^2 - \mu^2)(p^2 - \nu^2)}{p^2(p^2 - q^2)}\right]^{\frac{1}{2}}, \quad Y = \left[\frac{(\lambda^2 - q^2)(\mu^2 - q^2)(q^2 - \nu^2)}{(p^2 - q^2)q^2}\right]^{\frac{1}{2}}, \quad Z = \frac{\lambda\mu\nu}{pq}.$$

Here the constants $p$ and $q$ take values so that $0 < \nu < q < \mu < p < \lambda < \infty$; surfaces of constant $\lambda$ are ellipsoids. We denote the free boundary $\Omega_0$ by $\lambda = \lambda_0$, so it is given by

$$\frac{X^2}{\lambda_0^2 - p^2} + \frac{Y^2}{\lambda_0^2 - q^2} + \frac{Z^2}{\lambda_0^2} = 1. \tag{26}$$

We also note that $R^2 = X^2 + Y^2 + Z^2 = \lambda^2 + \mu^2 + \nu^2 - p^2 - q^2$, so we have $R \sim \lambda$ as $\lambda \to \infty$.

Now, in ellipsoidal coordinates

$$aX^2 + bY^2 + (\tfrac{1}{2} - a - b)Z^2 = F_1(\lambda) + F_2(\lambda)\mu^2\nu^2 + F_3(\lambda)(\mu^2 + \nu^2), \tag{27}$$

where

$$F_1 = \frac{(ap^2 - bq^2)\lambda^2 - ap^4 + bq^4}{p^2 - q^2}, \quad F_2 = \frac{[(\frac{1}{2} - 2b - a)p^2 - (\frac{1}{2} - 2a - b)q^2]\lambda^2 - (a - b)p^2q^2}{p^2q^2(p^2 - q^2)},$$

$$F_3 = \frac{-(a-b)\lambda^2 + ap^2 - bq^2}{p^2 - q^2}.$$

The boundary-value problem for $\Phi$ can be written as

$$\frac{h_2h_3}{h_1}\left[\frac{\partial^2\Phi}{\partial\lambda^2} + \frac{\lambda(2\lambda^2 - p^2 - q^2)}{(\lambda^2 - p^2)(\lambda^2 - q^2)}\frac{\partial\Phi}{\partial\lambda}\right] + \frac{h_3h_1}{h_2}\left[\frac{\partial^2\Phi}{\partial\mu^2} - \frac{\mu(2\mu^2 - p^2 - q^2)}{(p^2 - \mu^2)(\mu^2 - q^2)}\frac{\partial\Phi}{\partial\mu}\right]$$

$$+\frac{h_1h_2}{h_3}\left[\frac{\partial^2\Phi}{\partial\nu^2} + \frac{\nu(2\nu^2 - p^2 - q^2)}{(p^2 - \nu^2)(q^2 - \nu^2)}\frac{\partial\Phi}{\partial\nu}\right] = h_1h_2h_3, \tag{28}$$

with

$$\Phi = \frac{\partial\Phi}{\partial\lambda} = 0 \quad \text{on} \quad \lambda = \lambda_0 \tag{29}$$

and

$$\Phi \sim F_1(\lambda) + F_2(\lambda)\mu^2\nu^2 + F_3(\lambda)(\mu^2 + \nu^2) - d + \frac{1}{3\lambda} + O(\lambda^{-3}) \quad \text{as} \quad \lambda \to \infty. \tag{30}$$

Here the $h_i$ are scale factors defined by

$$h_1 = \left[\frac{(\lambda^2 - \mu^2)(\lambda^2 - \nu^2)}{(\lambda^2 - p^2)(\lambda^2 - q^2)}\right]^{\frac{1}{2}}, \quad h_2 = \left[\frac{(\lambda^2 - \mu^2)(\mu^2 - \nu^2)}{(p^2 - \mu^2)(\mu^2 - q^2)}\right]^{\frac{1}{2}}, \quad h_3 = \left[\frac{(\lambda^2 - \nu^2)(\mu^2 - \nu^2)}{(p^2 - \nu^2)(q^2 - \nu^2)}\right]^{\frac{1}{2}}.$$

The form of (27) suggests we look for a solution of the form

$$\Phi = f_1(\lambda) + f_2(\lambda)\mu^2\nu^2 + f_3(\lambda)(\mu^2 + \nu^2).$$

After substituting this into (28) we find, after some algebra, that the functions $f_1$, $f_2$ and $f_3$ satisfy the three coupled second-order ODEs

$$(\lambda^2 - p^2)(\lambda^2 - q^2)f_1'' + \lambda(2\lambda^2 - p^2 - q^2)f_1' + 2p^2q^2\lambda^2 f_2 + [4(p^2 + q^2)\lambda^2 - 2p^2q^2]f_3 = \lambda^4, \tag{31}$$

$$(\lambda^2 - p^2)(\lambda^2 - q^2)f_2'' + \lambda(2\lambda^2 - p^2 - q^2)f_2' + [4(p^2 + q^2) - 6\lambda^2]f_2 + 6f_3 = 1, \tag{32}$$

$$(\lambda^2 - p^2)(\lambda^2 - q^2)f_3'' + \lambda(2\lambda^2 - p^2 - q^2)f_3' - 2p^2q^2 f_2 - 6\lambda^2 f_3 = -\lambda^2, \tag{33}$$

where the dashes denote derivatives with respect to $\lambda$. Particular integrals are given by (27), namely $f_{1P} = F_1$, $f_{2P} = F_2$ and $f_{3P} = F_3$. The difficulty is with the complementary functions $f_{1H}$, $f_{2H}$, $f_{3H}$, which satisfy (31)-(33) with the right-hand sides set to zero. Before we solve these equations it is instructive to note that in all we will have nine unknowns. These are $p$, $q$, $\lambda_0$ and the two constants of integration in each of $f_{1H}$, $f_{2H}$ and $f_{3H}$ ($k_1$-$k_6$ in appendix A). The boundary conditions (29) and (30) give us the nine conditions

$$f_1 = f_1' = f_2 = f_2' = f_3 = f_3' = 0 \quad \text{on} \quad \lambda = \lambda_0, \tag{34}$$

$$f_{1H} = -d + \frac{1}{3\lambda} + O(\lambda^{-3}), \quad f_{2H} = O(\lambda^{-3}), \quad f_{3H} = O(\lambda^{-3}) \quad \text{as} \quad \lambda \to \infty. \tag{35}$$

Since $f_{1H}$ decouples, we solve for it last. The details of the solution process are given in appendix A, the resulting solutions being

$$f_{1H} = -\frac{(p^2+q^2)\sqrt{(\lambda^2-p^2)(\lambda^2-q^2)}}{2(p^2-q^2)^2\lambda} - \frac{(3\lambda^2-p^2-2q^2)F(\varphi,q/p)}{6p(p^2-q^2)}$$
$$+\frac{p(2\lambda^2-p^2-q^2)E(\varphi,q/p)}{2(p^2-q^2)^2} + \frac{1}{3p}F(\varphi,q/p) + k_6, \tag{36}$$

$$f_{2H} = -\frac{(p^2+q^2)\sqrt{(\lambda^2-p^2)(\lambda^2-q^2)}}{2p^2q^2(p^2-q^2)^2\lambda} - \frac{[(2p^2-q^2)\lambda^2-p^2q^2]F(\varphi,q/p)}{2p^3q^4(p^2-q^2)}$$
$$+\frac{[2(p^4-p^2q^2+q^4)\lambda^2-p^2q^2(p^2+q^2)]E(\varphi,q/p)}{2p^3q^4(p^2-q^2)^2}, \tag{37}$$

$$f_{3H} = \frac{\sqrt{(\lambda^2-p^2)(\lambda^2-q^2)}}{(p^2-q^2)^2\lambda} + \frac{(\lambda^2-q^2)F(\varphi,q/p)}{2pq^2(p^2-q^2)} - \frac{[(p^2+q^2)\lambda^2-2p^2q^2]E(\varphi,q/p)}{2pq^2(p^2-q^2)^2}, \tag{38}$$

where $\varphi = \arcsin(p/\lambda)$. Here $F(\varphi,k)$ and $E(\varphi,k)$ are, respectively, elliptic integrals of the first and second kind, defined by

$$F(\varphi,k) = \int_0^{\sin\varphi} \frac{dt}{\sqrt{(1-t^2)(1-k^2t^2)}} \quad \text{and} \quad E(\varphi,k) = \int_0^{\sin\varphi} \sqrt{\frac{1-k^2t^2}{1-t^2}}\, dt. \tag{39}$$

The remaining constants $p$, $q$, $\lambda_0$ and $d$ can be expressed in terms of $a$ and $b$ by the relations

$$a = \frac{\lambda_0^2-q^2}{2(p^2-q^2)} - \frac{E(\varphi_0,q/p)}{2p(p^2-q^2)}, \quad b = -\frac{\lambda_0^2-p^2}{2(p^2-q^2)} - \frac{F(\varphi_0,q/p)}{2pq^2} + \frac{pE(\varphi_0,q/p)}{2q^2(p^2-q^2)}, \tag{40}$$

$$\lambda_0\sqrt{(\lambda_0^2-p^2)(\lambda_0^2-q^2)} = 1, \quad d = F(\varphi_0,q/p)/2p. \tag{41}$$

Here $\varphi_0 = \arcsin(p/\lambda_0)$, and the free boundary is given by (26). Note that the first equation in (41) corresponds to $\Omega_0$ having volume $4\pi/3$, as required. It thus follows (by uniqueness of the solution to (16)-(18)) that the bubble is ellipsoidal in shape just before extinction.

The function $\Phi$ is related to the Newtonian gravity potential. We set $\Phi = 0$ inside $\Omega_0$ and define a new function $\hat{\Phi}$ by

$$\hat{\Phi} = aX^2 + bY^2 + (\tfrac{1}{2}-a-b)Z^2 - d - \Phi. \tag{42}$$

Clearly $\hat{\Phi}$ and its first derivatives are continuous throughout $\mathbb{R}^3$. Also, $\hat{\Phi}$ must satisfy

$$\frac{\partial^2\hat{\Phi}}{\partial X^2} + \frac{\partial^2\hat{\Phi}}{\partial Y^2} + \frac{\partial^2\hat{\Phi}}{\partial Z^2} = \begin{cases} 1 & \text{inside} \quad \Omega_0 \\ 0 & \text{outside} \quad \Omega_0 \end{cases}$$

as well as the condition

$$\hat{\Phi} \sim -\frac{1}{3R} + O(R^{-3}) \quad \text{as} \quad R \to \infty.$$

Therefore $\hat{\Phi}$ is simply the (non-dimensional) gravity potential of $\Omega_0$, given by

$$\hat{\Phi} = -\frac{1}{4\pi} \int_{\Omega_0} \frac{dX'dY'dZ'}{\sqrt{(X-X')^2 + (Y-Y')^2 + (Z-Z')^2}}. \tag{43}$$

Using the definition (43), it is possible to compute the gravity potential for an ellipsoid (see Chandrasekhar [3], for example) and after rescaling, recover the result (42) for $\Omega_0$. Note that $\Phi = 0$ inside $\Omega_0$ corresponds to the well-known result that the gravitational potential inside an ellipsoid is a simple quadratic.

Given the solution $\Phi$, we can now compute the function

$$\Psi(X, Y, Z) = \frac{1}{p}(F(\varphi, q/p) - F(\varphi_0, q/p)),$$

which was introduced in (21). A combination of (20) and (24) then leads to the result

$$u \sim 1 - \frac{F(\varphi, q/p)}{F(\varphi_0, q/p)} \quad \text{as} \quad T \to 0 \tag{44}$$

for the pressure in the inner region $r = O(T)$. This result is similar to that found by Howison [9], who in effect considered the time-reversal of our inner problem (with the added restriction that the bubble grows at a constant rate). Howison specifies the aspect ratios of the ellipsoidal free boundary in advance, and then determines the relevant solution by assuming pressure is a function of $\lambda$ only, while in the current problem the aspect ratios are determined by the matching conditions at infinity. Note that a function of $\lambda$ only, $\zeta(\lambda)$ say, satisfies Laplace's equation if

$$\frac{d^2\zeta}{d\lambda^2} + \frac{\lambda(2\lambda^2 - p^2 - q^2)}{(\lambda^2 - p^2)(\lambda^2 - q^2)} \frac{d\zeta}{d\lambda} = 0,$$

in which case it is of the form

$$\zeta = A\, F(\varphi, q/p) + B,$$

where $A$ and $B$ are constants.

It proves interesting to consider the aspect ratios of the free boundary as it evolves. We therefore define $r_{yx}(t)$ as the ratio of the bubble's axis in the $y$ direction to that in the $x$ direction, and $r_{zy}(t)$ as the ratio of the axis in the $z$ direction to that in the $y$ direction. The third aspect ratio can be defined in a similar way, and can be found from $r_{zx}(t) = r_{yx}(t) r_{zy}(t)$.

Just before extinction, these aspect ratios are those of the limiting ellipse (26), and we write

$$r^e_{yx} = \lim_{t\to t_e^-} r_{yx}(t) = \sqrt{\frac{\lambda_0^2 - q^2}{\lambda_0^2 - p^2}}, \quad r^e_{zy} = \lim_{t\to t_e^-} r_{zy}(t) = \frac{\lambda_0}{\sqrt{\lambda_0^2 - q^2}}. \tag{45}$$

Since $q < p < \lambda_0$, the limiting ellipsoid's axis in the $z$ direction is the longest, while that in the $x$ direction is shortest. It follows that both $r^e_{yx}$ and $r^e_{zy}$ are greater than unity. We also define aspect ratios at $t = 0$ by

$$r^0_{yx} = r_{yx}(0), \quad r^0_{zy} = r_{zy}(0),$$

and note that these two quantities are most meaningful if the domain $B$ is symmetrical. We now address some limiting cases in which the above results simplify significantly.

## 3.4 Special cases

### 3.4.1 The two-dimensional case

In the limit $\lambda_0 \to \infty$ with $p, q \to \infty$, the problem becomes two-dimensional in the $xy$-plane, and $b = \frac{1}{2} - a$. From (41) we see that

$$q^2 \sim \lambda_0^2 - \frac{c}{\lambda_0} + O(\lambda_0^{-2}), \quad p^2 \sim \lambda_0^2 - \frac{1}{c\lambda_0} + O(\lambda_0^{-2}) \quad \text{as} \quad \lambda_0 \to \infty, \tag{46}$$

where, from (40), $c = 2a/(1-2a)$. The expressions in (46) also imply the aspect ratio $r^e_{yx} \to c$ as $\lambda_0 \to \infty$, so we have the two-dimensional result

$$r^e_{yx} = \frac{2a}{1-2a}. \tag{47}$$

This result is applicable to bubble contraction in a Hele-Shaw cell, and can also be derived using modified gravity potentials, as suggested by Entov and Etingof [6].

From (41) we find that

$$d \sim \frac{1}{4\lambda_0}(3\log\lambda_0 + O(1)) \quad \text{as} \quad \lambda_0 \to \infty,$$

so the result (25) is no longer applicable in this limit. The rate at which two-dimensional bubbles contract (at times just before extinction) can be derived directly by reformulating the problem in an analogous way to that done in section 3, where now the initial geometry $B$ is an infinite cylinder whose cross-section lies parallel to the $xy$-plane. The details are given in

appendix B, but the result is that if we define the area of the cross-section of $\Omega(t)$ to be $\pi\bar{T}^2$, then the rate at which $\bar{T}$ decreases is given asymptotically by

$$\bar{T} \sim \frac{2(t_e - t)^{1/2}}{\log^{1/2}(1/(t_e - t))} \left[1 - \frac{\log\log(1/(t_e - t)) + 1 + \log[2a(1-2a)] - 2\bar{K}}{2\log(1/(t_e - t))}\right] \tag{48}$$

as $t \to t_e^-$. Here the constant $\bar{K}$ depends on the geometry $\partial B$, and is determined by solving the linear boundary-value problem (80).

### 3.4.2 Prolate spheroids

When $b = a$ we have $q = p$ and the free boundary is a prolate spheroid. By taking the limit $q \to p$ in (40)-(41) we find

$$a = b = \frac{\lambda_0^3}{4(\lambda_0^3 - 1)} - \frac{\lambda_0^{3/2}}{8(\lambda_0^3 - 1)^{3/2}} \log\left[\frac{\lambda_0^{3/2} + (\lambda_0^3 - 1)^{1/2}}{\lambda_0^{3/2} - (\lambda_0^3 - 1)^{1/2}}\right], \tag{49}$$

$$p = q = \frac{(\lambda_0^3 - 1)^{1/2}}{\lambda_0^{1/2}}, \quad d = \frac{\lambda_0^{1/2}}{4(\lambda_0^3 - 1)^{1/2}} \log\left[\frac{\lambda_0^{3/2} + (\lambda_0^3 - 1)^{1/2}}{\lambda_0^{3/2} - (\lambda_0^3 - 1)^{1/2}}\right]. \tag{50}$$

The free boundary is given by $\lambda_0(X^2 + Y^2) + Z^2/\lambda_0^2 = 1$, while the aspect ratios are given by $r_{yx}^e = 1$ and $r_{zy}^e = \lambda_0^{3/2}$. Note than when $\lambda_0 \to \infty$, the free boundary approaches the circular cylinder $X^2 + Y^2 = \lambda_0^{-1}$, which is also a special case of the previous subsection and has $a \to \frac{1}{4}^-$ and $d \to 0^+$. Exact results for this limit are given at the end of appendix B.

### 3.4.3 Oblate spheroids

When $b = \frac{1}{4}(1 - 2a)$ we have $q = 0$ and the free boundary becomes the oblate spheroid $\lambda_0^4 X^2 + (Y^2 + Z^2)/\lambda_0^2 = 1$. In this case

$$a = \tfrac{1}{2} - 2b = \frac{\lambda_0^6}{2(\lambda_0^6 - 1)} - \frac{\lambda_0^6}{2(\lambda_0^6 - 1)^{3/2}} \arctan(\lambda_0^6 - 1)^{1/2}, \tag{51}$$

$$p = \frac{(\lambda_0^6 - 1)^{1/2}}{\lambda_0^2}, \quad d = \frac{\lambda_0^2}{2(\lambda_0^6 - 1)^{1/2}} \arctan(\lambda_0^6 - 1)^{1/2}, \tag{52}$$

with aspect ratios $r_{yx}^e = \lambda_0^3$ and $r_{zy}^e = 1$.

In the limit $\lambda_0 \to \infty$ (with $q = 0$) the solution becomes one-dimensional, with $a \to \frac{1}{2}^-$ and $d \to 0^+$. The result (25) is no longer applicable in this case, since the right-hand side becomes singular. We can, however, easily derive the appropriate result by solving (8)-(9)

exactly. Supposing the domain $B$ is given by $-L \le x \le L$, $-\infty < y < \infty$, $-\infty < z < \infty$, then the solution for $w(x,t)$ is

$$w = \tfrac{1}{2}x^2 - \tilde{T}(t)x + \tfrac{1}{2}\tilde{T}(t)^2, \quad t_e = \tfrac{1}{2}L^2, \quad x_e = 0,$$

where function $\tilde{T}(t)$, given by

$$\tilde{T}(t) = L - \sqrt{2t},$$

is the distance of the free boundary from the $yz$-plane.

### 3.4.4 Spherical symmetry

When $\lambda_0 \to 1^+$ in either (49)-(50) or (51)-(52) the spheroid approaches the unit sphere $X^2 + Y^2 + Z^2 = 1$, with $a = b \to \frac{1}{6}^+$ and $d \to -\frac{1}{2}^+$. The inner solution in this limit is simply

$$\Phi = \frac{1}{6}R^2 - \frac{1}{2} + \frac{1}{3R}. \tag{53}$$

When $\partial B$ is the sphere $x^2 + y^2 + z^2 = \alpha^2$, it is straightforward to solve (8)-(9) for all time. The result is

$$w(r,t) = \frac{1}{6}r^2 - \frac{1}{2}T^2 + \frac{1}{3r}T^3 = T^2\left(\frac{1}{6}R^2 - \frac{1}{2} + \frac{1}{3R}\right), \tag{54}$$

where the function $T$ is given implicitly by

$$t = \frac{1}{6}\alpha^2 - \frac{1}{2}T^2 + \frac{1}{3\alpha}T^3$$

and $R = r/T$. In this case $T$ is simply the radial distance of the free boundary to the origin and the leading-order inner solution (53) is in fact exact, since

$$w_e = \frac{1}{6}r^2, \quad t_e = \frac{1}{6}\alpha^2, \quad G = \frac{1}{4\pi}\left(\frac{1}{r} - \frac{1}{\alpha}\right).$$

## 3.5 Summary: free boundary description

In summary, to determine the behaviour of the free boundary at times leading up to extinction we need first to solve the boundary-value problem (10)-(11) for $W$, giving the values of the contants $a$ and $b$ with the use of (13). This process also yields the extinction time $t_e$ and the extinction point $\mathbf{x}_e$. The constants $\lambda_0$, $p$, $q$ and $d$ can be computed with the use of (40)-(41), with the shape of the limiting free boundary given by

$$\frac{x^2}{\lambda_0^2 - p^2} + \frac{y^2}{\lambda_0^2 - q^2} + \frac{z^2}{\lambda_0^2} = T^2. \tag{55}$$

Here $T$ is the function defined so that the volume of the bubble is $4\pi T^3/3$; its asymptotic behaviour as $t \to t_e^-$ is given by (25) (unless the geometry is strictly one or two-dimensional, in which case see sections 3.4.3 and 3.4.1, respectively), where the constant $K$ is determined by the boundary-value problem (23). We also note that a combination of (24) and (55) implies

$$\omega(x,y,z) \sim t_e - d\left[\frac{x^2}{\lambda_0^2 - p^2} + \frac{y^2}{\lambda_0^2 - q^2} + \frac{z^2}{\lambda_0^2}\right] + \frac{K}{3}\left[\frac{x^2}{\lambda_0^2 - p^2} + \frac{y^2}{\lambda_0^2 - q^2} + \frac{z^2}{\lambda_0^2}\right]^{3/2} \quad \text{as} \quad r \to 0.$$

In the next section we will apply this recipe to specific domain shapes, $B$.

# 4 Examples

**Example 1**. Perhaps the most instructive example is when the fixed boundary $\partial B$ is itself an ellipsoid, namely

$$x^2 + \frac{1}{\gamma^2}y^2 + \frac{1}{\delta^2}z^2 = 1, \tag{56}$$

with $1 \le \gamma \le \delta$. Here the solution to (10)-(11) implies that $w_e$ is simply given by

$$w_e = \frac{\gamma^2\delta^2}{2(\gamma^2 + \delta^2 + \gamma^2\delta^2)}\,x^2 + \frac{\delta^2}{2(\gamma^2 + \delta^2 + \gamma^2\delta^2)}\,y^2 + \frac{\gamma^2}{2(\gamma^2 + \delta^2 + \gamma^2\delta^2)}\,z^2,$$

with

$$t_e = \frac{\gamma^2\delta^2}{2(\gamma^2 + \delta^2 + \gamma^2\delta^2)}, \quad \mathbf{x}_e = \mathbf{0}.$$

It follows that the constants $a$ and $b$ appearing in (13) are given by

$$a = \frac{\gamma^2\delta^2}{2(\gamma^2 + \delta^2 + \gamma^2\delta^2)}, \quad b = \frac{\delta^2}{2(\gamma^2 + \delta^2 + \gamma^2\delta^2)}.$$

For $t \ll 1$, the leading order behaviour in the boundary layers in which the normal distance from $\partial B$ is $O(t^{1/2})$ is one-dimensional, and it follows that the free boundary $\partial\Omega$ is described by

$$x^2 + \frac{1}{\gamma^2}y^2 + \frac{1}{\delta^2}z^2 \sim 1 - 2\sqrt{2t}\left(x^2 + \frac{1}{\gamma^4}y^2 + \frac{1}{\delta^4}z^2\right)^{1/2} \quad \text{as} \quad t \to 0^+,$$

and that the aspect ratios have the behaviour

$$r_{yx} \sim \gamma + (\gamma - 1)\sqrt{2t}, \quad r_{zy} \sim \frac{\delta}{\gamma} + \frac{\delta - \gamma}{\gamma^2}\sqrt{2t} \quad \text{as} \quad t \to 0^+.$$

In follows in particular that the bubble does *not* retain its ellipsoidal shape when contracting to the origin. Instead, the free boundary evolves from its initial shape until it again approaches an ellipsoidal shape at extinction. The aspect ratios $r_{yx}$ and $r_{zy}$ increase for small time and we

also find that $r^e_{yx}$ and $r^e_{zy}$ defined in (45) are greater than $r^0_{yx} = \gamma$ and $r^0_{zy} = \delta/\gamma$ respectively; we expect $r_{yx}$ and $r_{zy}$ to be monotone increasing.

The relationships between the aspect ratios of the ellipsoidal free boundary near extinction and those of the fixed ellipsoid (56) are illustrated in Figures 1 and 2. To obtain this data we have to evaluate the elliptic integrals in (40), which has been done using NAG routines. In Figure 1, typical plots of $r^e_{zy}/r^0_{zy}$ versus $\delta$ are shown for differing values of $\gamma$. It is immediately clear that the aspect ratio $r^e_{zy}$ of the ellipsoidal free boundary near extinction is greater than the corresponding aspect ratio $r^0_{zy} = \delta/\gamma$ of the fixed ellipsoid for all values of $\gamma$ and $\delta$; furthermore, as $\delta$ increases along these curves, we see that $r^e_{zy}$ increases faster than $r^0_{zy}$, indicating that the distinction between the two aspect ratios becomes more pronounced as we stretch the fixed ellipsoid.

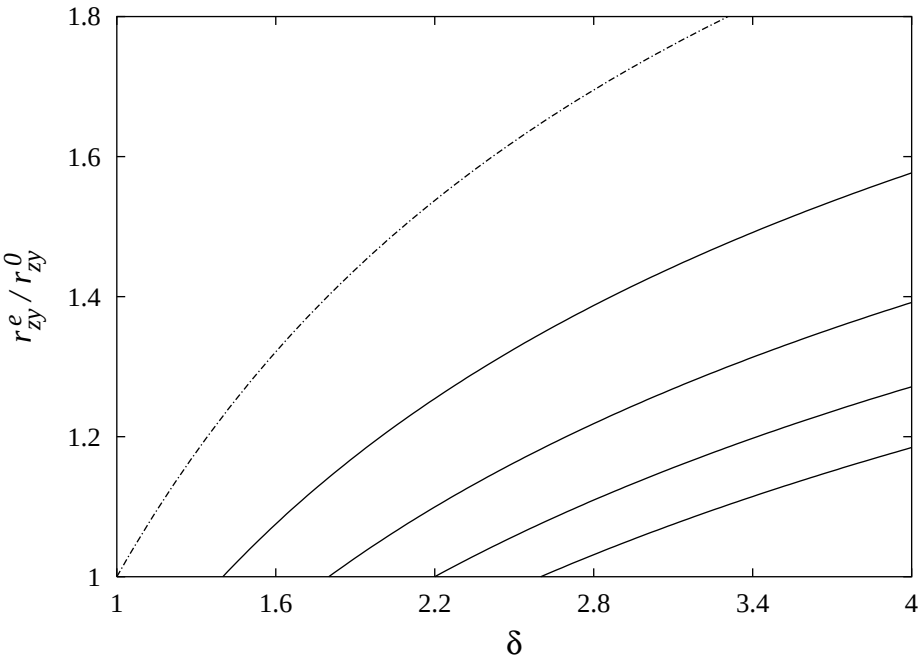


Figure 1: The dependence of the quotient $r^e_{zy}/r^0_{zy}$ on $\delta$ for the case in which $\partial B$ is the ellipsoid $x^2 + y^2/\gamma^2 + z^2/\delta^2 = 1$. The dot-dashed line had $\gamma = 1$ (prolate spheroid), while from left to right, the solid curves have $\gamma = 1.4$, 1.8, 2.2 and 2.6. The curve for $\gamma = \delta$ (oblate spheroid) is simply the $\delta$-axis.

In Figure 2 we show the dependence of $r^e_{yx}/r^0_{yx}$ on $\delta$. Again, with the exception of the case $\gamma = 1$, we see that the aspect ratio $r^e_{yx}$ of the ellipsoidal free boundary near extinction is greater than the corresponding aspect ratio $r^0_{yx} = \gamma$ of the fixed boundary. Note that these curves

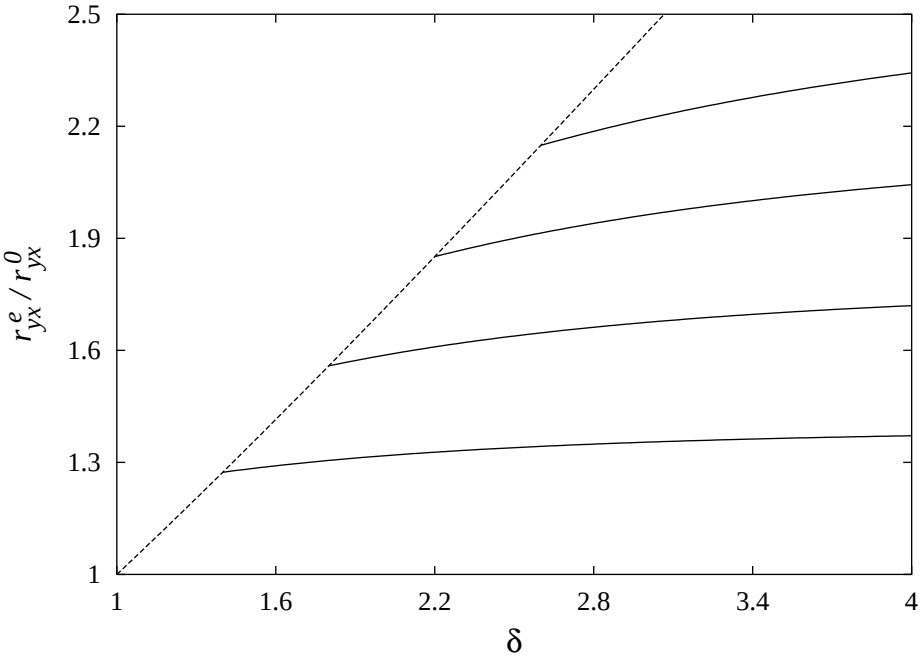


Figure 2: The dependence of the quotient $r^e_{yx}/r^0_{yx}$ on $\delta$ for the case in which $B$ is the ellipsoid $x^2 + y^2/\gamma^2 + z^2/\delta^2 = 1$. The curve for $\gamma = 1$ (prolate spheroid) is the $\delta$-axis, while from bottom to top, the solid curves have $\gamma = 1.4$, 1.8, 2.2 and 2.6. The dashed line has $\gamma = \delta$ (oblate spheroid).

again increase monotonically with $\delta$. This means the aspect ratio $r^e_{yx}$ increases even though the dimensions of the fixed geometry in the $x$ and $y$ directions remain constant. In fact in this example we know that $r^e_{yx}/r^0_{yx} \to \gamma$ as $\delta \to \infty$; this is the two-dimensional limit, computed with the use of (47).

The behaviour of the free boundary in this example should be contrasted with that of a bubble contracting in an infinite domain. Here, if the bubble is initially ellipsoidal, then it remains so, with constant aspect ratios (cf. Entov and Etingof [6]), as it evolves.

**Example 2**. Now suppose $B$ is the cuboid $-1 \le x \le 1$, $-\gamma \le y \le \gamma$, $-\delta \le z \le \delta$, with $1 \le \gamma \le \delta$. We can use separation of variables to solve (10) for $W$ which, along with (11), yields $w_e = t_e + \frac{1}{2}(z^2 - \delta^2) + \chi_1(x, y, z) + \chi_2(x, y, z)$, where

$$\chi_1 = \sum_{m=0}^{\infty}\sum_{n=0}^{\infty} A_{mn} \cosh(\alpha_{mn} x) \cos\left[\frac{(2m+1)\pi y}{2\gamma}\right] \cos\left[\frac{(2n+1)\pi z}{2\delta}\right],$$

$$\chi_2 = \sum_{m=0}^{\infty}\sum_{n=0}^{\infty} B_{mn} \cos\left[\frac{(2m+1)\pi x}{2}\right] \cosh(\beta_{mn} y) \cos\left[\frac{(2n+1)\pi z}{2\delta}\right],$$

as well as the the extinction time

$$t_e = \tfrac{1}{2}\delta^2 - \sum_{m=0}^{\infty}\sum_{n=0}^{\infty}\left\{\frac{64\delta^2(-1)^{m+n}}{\pi^4(2m+1)(2n+1)^3}\left(\frac{1}{\cosh\alpha_{mn}} + \frac{1}{\cosh(\beta_{mn}\gamma)}\right)\right\}; \tag{57}$$

we have $\mathbf{x}_e = \mathbf{0}$ by symmetry. Here we have used the constants

$$A_{mn} = \frac{64\delta^2(-1)^{m+n}}{\pi^4(2m+1)(2n+1)^3\cosh\alpha_{mn}}, \quad B_{mn} = \frac{64\delta^2(-1)^{m+n}}{\pi^4(2m+1)(2n+1)^3\cosh(\beta_{mn}\gamma)},$$

$$\alpha_{mn} = \left[\frac{\pi^2}{4\delta^2}(2n+1)^2 + \frac{\pi^2}{4\gamma^2}(2m+1)^2\right]^{1/2}, \quad \beta_{mn} = \left[\frac{\pi^2}{4\delta^2}(2n+1)^2 + \frac{\pi^2}{4}(2m+1)^2\right]^{1/2}.$$

The behaviour of $w_e$ near the origin also yields the constants

$$a = \sum_{m=0}^{\infty}\sum_{n=0}^{\infty}\left\{\frac{8\delta^2(-1)^{m+n}}{\pi^2(2m+1)(2n+1)^3}\left[\frac{(2m+1)^2}{\gamma^2\cosh\alpha_{mn}} - \frac{(2m+1)^2}{\cosh(\beta_{mn}\gamma)} + \frac{(2n+1)^2}{\delta^2\cosh\alpha_{mn}}\right]\right\}, \tag{58}$$

$$b = \sum_{m=0}^{\infty}\sum_{n=0}^{\infty}\left\{\frac{8\delta^2(-1)^{m+n}}{\pi^2(2m+1)(2n+1)^3}\left[\frac{(2m+1)^2}{\cosh(\beta_{mn}\gamma)} - \frac{(2m+1)^2}{\gamma^2\cosh\alpha_{mn}} + \frac{(2n+1)^2}{\delta^2\cosh(\beta_{mn}\gamma)}\right]\right\}. \tag{59}$$

We note that the double sums in (57)-(59) converge rapidly and that only a few terms are needed in each case to obtain an accurate numerical approximation.

In Figures 3 and 4 typical plots of the quotients $r^e_{zy}/r^0_{zy}$ and $r^e_{yx}/r^0_{yx}$ versus the length $\delta$ are presented for the current example. These figures are analogous to Figures 1 and 2, and it is clear that the qualitative behaviour is the same regardless of the initial geometry. It is noteworthy that in this example these quotients are surprisingly large.

The dependence of the extinction time $t_e$ on $\delta$ is presented in Figure 5 for both the case where $\partial B$ is given by (56) and for the current example. The dot-dashed line in Figure 5(a), for which $\partial B$ is a prolate spheroid, begins at the point where $\partial B$ is the unit sphere, with $t_e = \frac{1}{6}$. As $\delta$ increases on this curve the spheroid stretches and approaches a unit circular cylinder as $\delta \to \infty$, with $t_e \to \frac{1}{4}$ in this limit. Similarly, as $\delta$ increases along each of the solid curves the fixed boundary $\partial B$ approaches an elliptic cylinder and the solutions becomes two-dimensional; here $t_e \to \gamma^2/2(1+\gamma^2)$ as $\delta \to \infty$. Finally, the dashed curve, where $\partial B$ is an oblate spheroid, has the spheroid becoming flatter in shape as $\delta$ increases; the solution becomes one-dimensional as $\delta \to \infty$, and the free boundary propagates with speed $1/\sqrt{2t}$, with $t_e \to \frac{1}{2}$ as $\gamma = \delta \to \infty$. It is easy to see that the qualitative behaviour in (b) is the same as that shown in (a). Of course, for given $\gamma$ and $\delta$, we expect the extinction times for the current example to be greater than in the previous one, and this behaviour is confirmed by the figures.

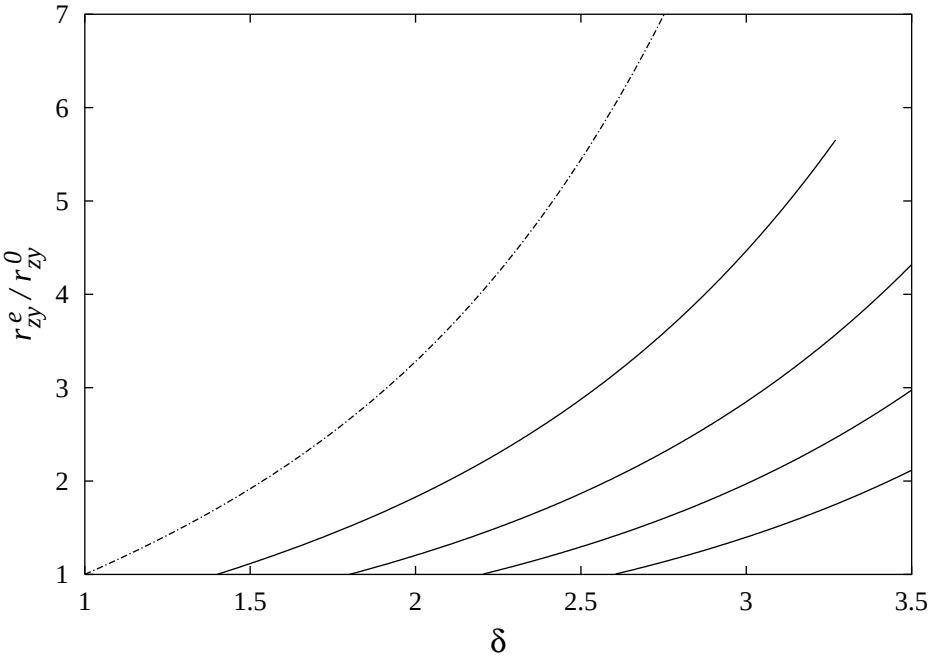


Figure 3: The dependence of the quotient $r^e_{zy}/r^0_{zy}$ on $\delta$ for the case in which $B$ is the cuboid $-1 \leq x \leq 1$, $-\gamma \leq y \leq \gamma$, $-\delta \leq z \leq \delta$. The dot-dashed line is for $\gamma = 1$ while, from left to right, the solid curves are drawn for $\gamma = 1.4$, 1.8, 2.2 and 2.6. The curve for $\gamma = \delta$ is the $\delta$-axis.

# 5 Discussion

In this paper we have studied the contraction of a bubble in a porous medium filled with viscous fluid. By formulating the problem in terms of a Baiocchi transformed variable and analysing the resulting equations using matched asymptotic expansions, we have been able to describe the behaviour at times just before bubble extinction. The advantage of using the Baiocchi transform is that time appears only as a parameter in the problem; we can find the precise extinction behaviour without solving the full initial-boundary-value problem.

The extinction behaviour for the bubble contraction problem is *not* radially symmetric, as one might first imagine. Instead, the bubble becomes ellipsoidal in shape as it approaches extinction, regardless of the initial geometry. By solving the inner problem in ellipsoidal coordinates, we have found how the dimensions of the ellipsoid, *and* the rate at which it vanishes, depend on three constants ($a$, $b$ and $K$) which characterise the domain (via the solution to (10)-(11) and (23)). Moreover, the nature of the extinction behaviour is also independent of the boundary conditions on $\partial B$, though these influence the values of $a$, $b$ and $K$ through the appropriate modifications to (10)-(11), (23).

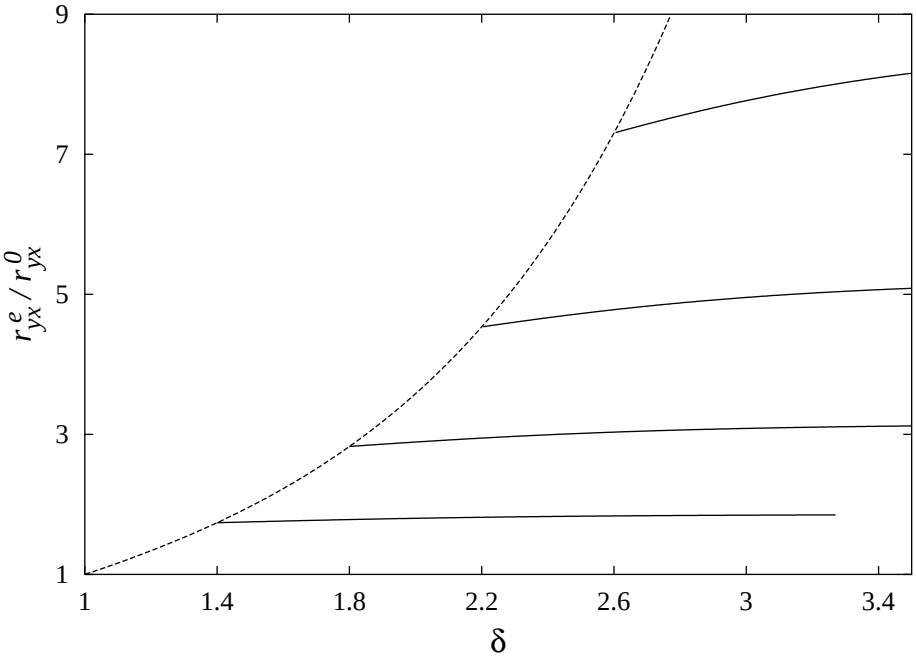


Figure 4: The dependence of the quotient $r^e_{yx}/r^0_{yx}$ on $\delta$ for the case in which $B$ is the cuboid $-1 \leq x \leq 1$, $-\gamma \leq y \leq \gamma$, $-\delta \leq z \leq \delta$. The curve for $\gamma = 1$ is the $\delta$-axis while, from bottom to top, the solid curves have $\gamma = 1.4$, 1.8, 2.2 and 2.6 and the dashed line has for $\gamma = \delta$.

In our analysis we have tried to give a detailed and clear account of the various steps used to compute the point at which the bubble vanishes, the time it takes to vanish, and the aspect ratios of the limiting (ellipsoidal) boundary. These results for $B \subset \mathbb{R}^3$ extend those presented by Entov and Etingof [6] for $B \subset \mathbb{R}^2$, and in fact the formulas to compute $\mathbf{x}_e$ and $t_e$ generalise to $B \subset \mathbb{R}^N$ (see appendix C.2).

For the physical problem described by (1)-(3), it is clear that the bubble will only contract until $P_B = P_E$, at which point a steady state is reached. The results of our analysis imply that if $P_E \gg P_B$ then this steady state will be a small, approximately ellipsoidal bubble.

It is shown by examples (in section 4) that the aspect ratios of the free boundary near extinction can be quite different from those of the initial geometry, this difference being much greater in the second example when the fixed geometry is a cuboid. For instance, if we have a cuboid the length of whose sides is in the ratio 1:1.5:3, then the corresponding ratios for the ellipsoidal free boundary near extinction are 1:3.17:24.94. This surprising result suggests that a little stretching of the initial fixed domain can quickly produce long, slender ellipsoidal bubbles near extinction.

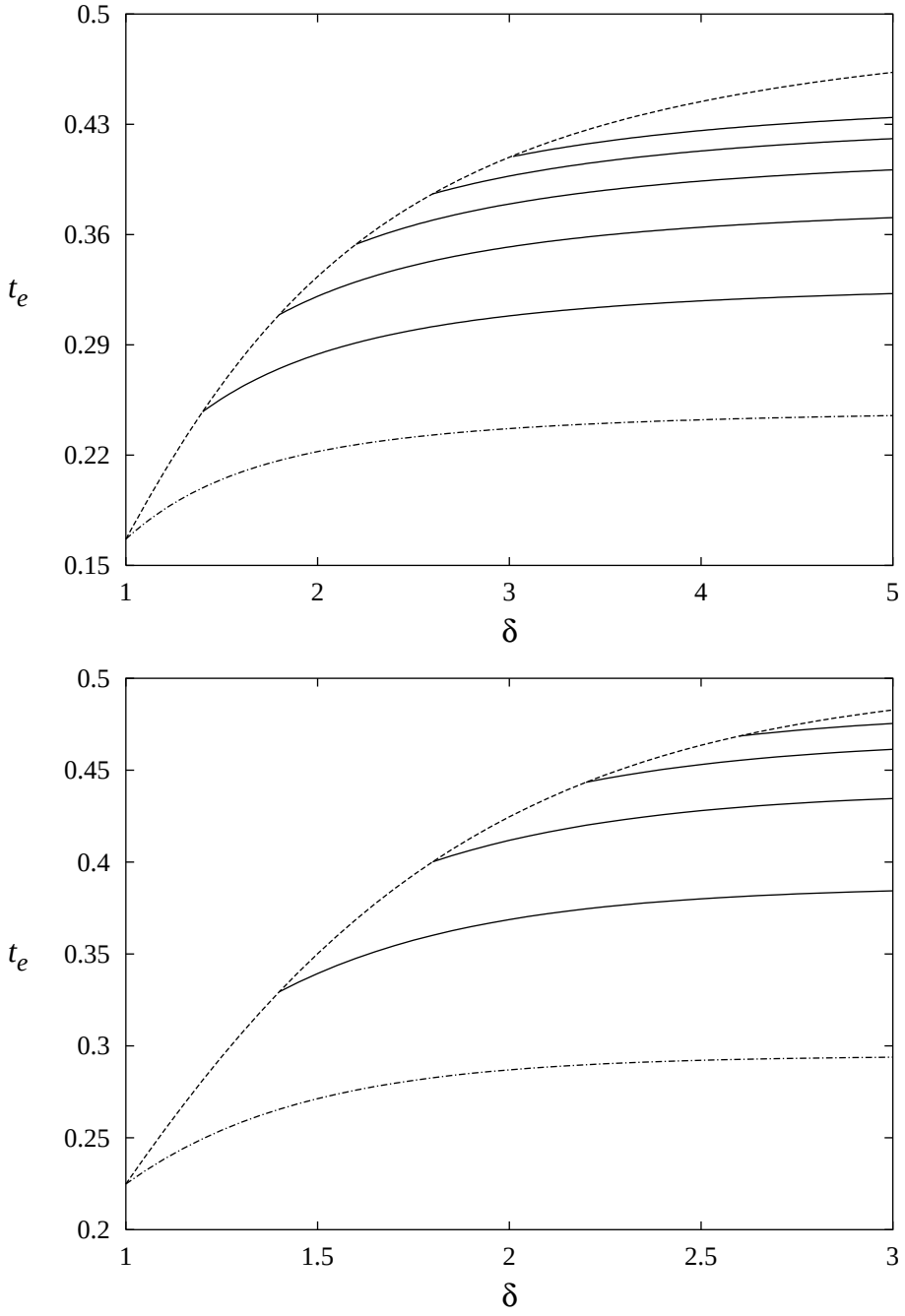


Figure 5: The dependence of the extinction time $t_e$ on $\delta$ for (a) the case where $\partial B$ is the ellipsoid $x^2 + y^2/\gamma^2 + z^2/\delta^2 = 1$, and (b) the case in which $B$ is the cuboid $-1 \leq x \leq 1$, $-\gamma \leq y \leq \gamma$, $-\delta \leq z \leq \delta$. The dot-dashed lines represent data for $\gamma = 1$, while from bottom to top, the solid curves are drawn in each case for $\gamma = 1.4$, 1.8, 2.2, and 2.6 (the top one in (a) is for $\gamma = 3$). The dashed lines represent data for $\gamma = \delta$.

For the purposes of this study we have assumed that the bubble contracts to only one point. However this need not always be the case, and for non-convex boundaries $\partial B$ (whereby $w_e$ has

more than one local minimum) bubble break up may occur, leading to multiple extinction points. Either way, the qualitative behaviour near each extinction point should be the same as that described above, except in non-generic cases on the borderline between single and multiple extinction points, say.

Consideration of time-reversal raises some extra issues. As already noted, in the ill-posed case in which fluid is extracted at infinity, ellipsoidal bubbles are known to provide the only solutions which exist for all times in $\mathbb{R}^N$ (see Di Benedetto and Friedman [4]); the bubble can be nucleated at any location with any orientation and aspect ratios. The situation with finite domains is rather different; replacing (5) by $u = -1$ on $\partial B$ and writing

$$w(\mathbf{x}, t) = -\int_t^\omega u(\mathbf{x}, t')\, dt' \tag{60}$$

yields (8)-(9), except that the condition on $\partial B$ becomes

$$w = w_0(\mathbf{x}) - t \quad \text{on} \quad \partial B, \tag{61}$$

where $w_0 = w(\mathbf{x}, 0)$. Since

$$\nabla^2 w_0 = 1 \quad \text{in} \quad B \setminus \Omega(0), \tag{62}$$

if the bubble is present at $t = 0$, $w_0$ in (61) can be obtained by solving the Cauchy problem for (62) whereby

$$w_0 = \frac{\partial w_0}{\partial n} = 0 \quad \text{on} \quad \partial\Omega(0).$$

However, if nucleation has yet to occur no boundary conditions hold on (62) and one is free to specify $w_0$ on $\partial B$, so that serious non-uniqueness arises; $w_0$ should, however, be chosen such that $t^* \equiv \min_{\mathbf{x}\in B} w_0 \geq 0$, in which case a bubble will nucleate at $t = t^*$ (with $w = w_0 - t$ for $t \leq t^*$) at the point $\mathbf{x}_e$ at which $w_0$ attains its minimum in $\mathbf{x}$ and its orientation and aspect ratios can be expressed in terms of the local behaviour of $w_0$, as described above. However, unless

$$w_0(\mathbf{x}) = t^* + t_e \quad \text{on} \quad \partial B \tag{63}$$

holds then the solution must cease to exist before the bubble fills the whole domain $B$. If (63) holds (so that $w_0 = t^* + t_e + W(\mathbf{x})$ is defined uniquely up to the value $t^*$) then the solution for $t \geq t^*$ is given by that of (8)-(9) (in which $\Omega(0) = B$) with $t$ replaced by $t^* + t_e - t$, so at $t = t^* + t_e$ a domain-filling bubble whose initial form is (unlike in the infinite domain case, in which an ellipsoidal bubble corresponds to $w_0$ being an arbitrary quadratic solution to (62))

completely specified (via the local behaviour of $W(\mathbf{x})$ at $\mathbf{x} = \mathbf{x}_e$). Such 'domain-filling' solutions are of course unstable (reflecting the ill-posedness of the problem) and it is unclear whether they may be selected by suitable regularisations. A possible application for such bubble growth problems lies in geology, where there is interest in de-gassing events following depressurisation of load-bearing liquid-saturated rock.

It is worth generalising some of these considerations to ill-posed Stefan problems; we note that (unlike its quasi-steady limit $\beta = \infty$) the ill-posed Stefan problem is not the time-reversal of the well-posed one (which we shall address elsewhere) due to the time-derivative in the heat equation. We consider

$$\frac{1}{\beta}\frac{\partial u}{\partial t} = \nabla^2 u \quad \text{in} \quad B \setminus \Omega(t), \tag{64}$$

$$\frac{\partial u}{\partial n} = 0 \quad \text{on} \quad \partial B, \tag{65}$$

$$u = 0, \quad V_n = -\frac{\partial u}{\partial n} \quad \text{on} \quad t = \omega, \tag{66}$$

$$u = u_0(\mathbf{x}) \quad \text{at} \quad t = 0, \tag{67}$$

where $\beta > 0$ with

$$\int_B (\beta + u_0(\mathbf{x}))d\mathbf{x} = 0 \tag{68}$$

(so, interpreting $u$ as a temperature, there is precisely enough supercooling in the fluid to freeze the whole of $B$), and it is simplest for the purposes of this discussion to adopt Neumann boundary conditions in this context. The Baiocchi transform (60) now yields

$$\frac{1}{\beta}\frac{\partial w}{\partial t} = \nabla^2 w - 1 \quad \text{in} \quad B \setminus \Omega(t), \tag{69}$$

$$\frac{\partial w}{\partial n} = \frac{\partial w_0}{\partial n} \quad \text{on} \quad \partial B, \tag{70}$$

$$w = \frac{\partial w}{\partial n} = 0 \quad \text{on} \quad t = \omega, \tag{71}$$

$$w = w_0(\mathbf{x}) \quad \text{at} \quad t = 0, \tag{72}$$

where

$$\nabla^2 w_0 = 1 + u_0(\mathbf{x})/\beta \tag{73}$$

but, if the solid phase $\Omega(0)$ is initially absent, there are again no boundary conditions on $w_0$. Specifying $w_0$ such that $t^* \geq 0$, the boundary conditions on $t = \omega$ do not apply for $0 < t < t_c$, where $t_c$ is such that $\min_{\mathbf{x} \in B} w(\mathbf{x}, t_c) = 0$, since no solid phase is then present and a linear

diffusion problem results. At $t = t_c$ the solid phase nucleates at $\mathbf{x} = \mathbf{x}_c$, the point at which $w_c(\mathbf{x}) \equiv w(\mathbf{x}, t_c)$ attains its minimum of zero, presumably in the ellipsoidal self-similar form

$$w \sim (t - t_c)\Theta((\mathbf{x} - \mathbf{x}_c)/(t - t_c)^{1/2}) \tag{74}$$

where (as in Ham [8]), $\Theta$ satisfies an ordinary differential equation (whose solution determines the aspect ratios of the ellipsoid in terms of the quadratic terms in the Taylor expansion for $w_c(\mathbf{x})$ about $\mathbf{x} = \mathbf{x}_c$) in the appropriate ellipsoidal coordinate. If the solid phase is to fill the whole domain, at $t = t_f$, say, then $\omega(\mathbf{x}) = t_f$ for $\mathbf{x} \in \partial\Omega$ and $w \to 0$ as $t \to t_f^-$, so that

$$\frac{\partial w}{\partial n} = \frac{\partial w_0}{\partial n} = 0 \quad \text{on} \quad \partial B \tag{75}$$

must hold. Equations (73) and (75) determine $w_0$ only up to a constant (note the role of (68) here), corresponding to $t^*$; thus if we wish the solid phase to nucleate at $t = 0$ we require $\min_{\mathbf{x} \in B} w_0 = 0$ (implying $t^* = t_c = 0$), making $w_0$ completely specified. Again, unlike the infinite domain case, the initial behaviour of the 'domain-filling' nucleate can thus be completely characterised (via the local behaviour of $w_c(\mathbf{x})$, which is determined by linear problems). For other choices of $w_0$ (including cases in which some solid is present at $t = 0$ when one is not at liberty to prescibe $\partial w_0/\partial n$ on $\partial B$), blow-up will occur before the whole domain freezes. Finally, we note that the self-similar form (74) is not consistent with those which arise in related quasi-steady ($\beta = \infty$) problems in one and two dimensions, the limits $t \to t_c^+$ and $\beta \to \infty$ not commuting; the distinguised limit which gives the transition between the Stefan form (74) and the quasi-steady form (cf. section 3.4.3 and appendix B)) is not difficult to formulate, however.

# 6 Acknowledgements

The funding of the EPSRC is gratefully acknowledged.

# Appendix

## A Details of solution for $f_{1H}$, $f_{2H}$ and $f_{3H}$.

Here we solve for $f_{1H}$, $f_{2H}$ and $f_{3H}$ subject to the boundary conditions (34)-(35). These details are included to show how the solution to (16)-(18) can be derived from first principles without reference to the gravity potential (43).

By elimination of $f_{3H}$ between the homogeneous version of (32) and (33) we find

$$f_{2H}^{(4)} + \frac{6\lambda(2\lambda^2 - p^2 - q^2)}{(\lambda^2 - p^2)(\lambda^2 - q^2)} f_{2H}''' + \frac{3\lambda[8(\lambda^2 - p^2)(\lambda^2 - q^2) + (p^2 - q^2)^2]}{(\lambda^2 - p^2)^2(\lambda^2 - q^2)^2}(\lambda f_{2H}'' - f_{2H}') = 0, \quad (76)$$

a third order equation for $f_{2H}'$. Since $f_{2H}' = \lambda$ is a solution, we use reduction of order to find two other linearly independent solutions for $f_{2H}'$ by writing $f_{2H}' = \lambda g(\lambda)$ and substituting into (76); $g$ then satisfies

$$g''' + \frac{2[5\lambda^4 - 3(p^2 + q^2)\lambda^2 + p^2q^2]}{\lambda(\lambda^2 - p^2)(\lambda^2 - q^2)} g'' + \frac{3[4(\lambda^2 - p^2)(\lambda^2 - q^2)(4\lambda^2 - p^2 - q^2) + (p^2 - q^2)^2\lambda^2]}{(\lambda^2 - p^2)(\lambda^2 - q^2)} g' = 0,$$

with solution (found by MAPLE) $g = k_1 I_1(\lambda) + k_2 I_2(\lambda) + k_3$, where

$$I_1 = \int_\lambda^\infty \frac{dt}{[(t^2 - p^2)(t^2 - q^2)]^{3/2}} \quad \text{and} \quad I_2 = \int_\lambda^\infty \frac{dt}{t^2[(t^2 - p^2)(t^2 - q^2)]^{3/2}}.$$

The integrals can be evaluated with the help of Byrd and Friedman [1]. The results are

$$I_1 = \frac{2\lambda^2 - p^2 - q^2}{(p^2 - q^2)^2\lambda\sqrt{(\lambda^2 - p^2)(\lambda^2 - q^2)}} + \frac{F(\varphi, q/p)}{pq^2(p^2 - q^2)} - \frac{(p^2 + q^2)E(\varphi, q/p)}{pq^2(p^2 - q^2)^2},$$

$$I_2 = \frac{(p^2 + q^2)\lambda^2 - (p^4 + q^4)}{p^2q^2(p^2 - q^2)^2\lambda\sqrt{(\lambda^2 - p^2)(\lambda^2 - q^2)}} + \frac{(2p^2 - q^2)F(\varphi, q/p)}{p^3q^4(p^2 - q^2)} - \frac{2(p^4 - p^2q^2 + q^4)E(\varphi, q/p)}{p^3q^4(p^2 - q^2)^2},$$

where $\varphi = \arcsin(p/\lambda)$ and $F(\varphi, k)$ and $E(\varphi, k)$ are elliptic integrals defined by (39). After further integration we find that

$$f_{2H} = k_1 f_{21} - k_2 f_{22} + \tfrac{1}{2}k_3\lambda^2 + k_4,$$

where $f_{22}$ is the right-hand side of (37), and

$$f_{21} = \frac{\sqrt{(\lambda^2 - p^2)(\lambda^2 - q^2)}}{(p^2 - q^2)^2\lambda} + \frac{(\lambda^2 - q^2)F(\varphi, q/p)}{2pq^2(p^2 - q^2)} - \frac{[(p^2 + q^2)\lambda^2 - 2p^2q^2]E(\varphi, q/p)}{2pq^2(p^2 - q^2)^2}.$$

Using (32), it follows (again, after much algebra) that

$$f_{3H} = k_1 f_{31} - k_2 f_{32} - \tfrac{1}{6}k_3 p^2q^2 + k_4[\lambda^2 - \tfrac{2}{3}(p^2 + q^2)],$$

where $f_{32}$ is the right-hand side of (38), and

$$f_{31} = \frac{-(p^2+q^2)\sqrt{(\lambda^2-p^2)(\lambda^2-q^2)}}{2(p^2-q^2)^2\lambda} - \frac{[3\lambda^2-(p^2+2q^2)]F(\varphi,q/p)}{6p(p^2-q^2)} + \frac{p[2\lambda^2-(p^2+q^2)]E(\varphi,q/p)}{2(p^2-q^2)^2}.$$

It follows that

$$f_{2H} = \frac{1}{2}k_3\lambda^2 + k_4 - \frac{1}{15}k_1\lambda^{-3} + O(\lambda^{-5})$$

$$f_{3H} = k_4\lambda^2 - \frac{1}{6}k_3p^2q^2 - \frac{2}{3}k_4(p^2+q^2) + \left(\frac{2(p^2+q^2)}{45}k_1 + \frac{1}{15}k_2\right)\lambda^{-3} + O(\lambda^{-5})$$

as $\lambda \to \infty$, so by (35) we have $k_3 = k_4 = 0$.

With $k_3$ and $k_4$ determined, we now use (31) to find $f'_{1H}$. The result, after integration, is that

$$f_{1H} = k_1 f_{11} - k_2 f_{12} + \frac{k_5}{p}F(\varphi,q/p) + k_6,$$

where $f_{12}$ is the first three terms on the right-hand side of (36), and

$$f_{11} = \frac{(p^4+p^2q^2+q^4)\sqrt{(\lambda^2-p^2)(\lambda^2-q^2)}}{3(p^2-q^2)^2\lambda} + \frac{[3(p^2+2q^2)\lambda^2-(2p^4+3p^2q^2+4q^4)]F(\varphi,q/p)}{18p(p^2-q^2)} - \frac{p[3(p^2+q^2)\lambda^2-2(p^4+p^2q^2+q^4)]E(\varphi,q/p)}{6(p^2-q^2)^2}.$$

The far field behaviour of $f_{1H}$ is given by

$$f_{1H} = k_6 + k_5\lambda^{-1} + \left(-\frac{4p^4+5p^2q^2+4q^4}{135}k_1 - \frac{2(p^2+q^2)}{45}k_2 + \frac{p^2+q^2}{6}k_5\right)\lambda^{-3} + O(\lambda^{-5})$$

as $\lambda \to \infty$, so by (35) we require $k_5 = \frac{1}{3}$ and $k_6 = d$, where $d$ remains to be determined.

To evaluate the remaining constants $k_1$, $k_2$, $d$, $p$, $q$ and $\lambda_0$ in terms of $a$ and $b$, we enforce the six boundary conditions given in (34). It can be shown (by direct substitution) that $k_1 = 0$ and $k_2 = -1$, while the remaining are given implicitly by the relations (40)-(41).

# B The two-dimensional limit

Suppose $B$ is an infinite cylinder whose cross-section lies parallel to the $xy$-plane. The inner region is now $(x^2+y^2)^{1/2} = O(\bar{T}(t_e - t))$, where the function $\bar{T}$ is defined so that the area of the cross-section of $\Omega(t)$ is $\pi\bar{T}^2$. In the inner region we write $w \sim \bar{T}^2\bar{\Phi}(\bar{X},\bar{Y})$ as $\bar{T} \to 0$, where $\bar{X} = x/\bar{T}$ and $\bar{Y} = y/\bar{T}$, so that $\bar{\Phi}$ satisfies

$$\frac{\partial^2\bar{\Phi}}{\partial\bar{X}^2} + \frac{\partial^2\bar{\Phi}}{\partial\bar{Y}^2} = 1 \quad \text{outside} \quad \Omega_0, \quad \bar{\Phi} = \frac{\partial\bar{\Phi}}{\partial N} = 0 \quad \text{on} \quad \partial\Omega_0, \tag{77}$$

$$\bar{\Phi} \sim a\bar{X}^2 + (\tfrac{1}{2} - a)\bar{Y}^2 - \tfrac{1}{4}\log(\bar{X}^2 + \bar{Y}^2) + O(1) \quad \text{as} \quad \bar{X}^2 + \bar{Y}^2 \to \infty, \tag{78}$$

the solution to which is $\bar{\Phi} = A_1(\phi) + A_2(\phi)\cos 2\psi$, where

$$A_1 = \tfrac{1}{8}k^2(4a - 1 + \cosh 2\phi) - \tfrac{1}{2}\phi - \tfrac{1}{4}\log(1 - 4a) - \tfrac{1}{4}\,,$$

$$A_2 = \tfrac{1}{8}k^2(1 + (4a - 1)\cosh 2\phi) - \tfrac{1}{4}e^{-2\phi}\,, \quad k^2 = \frac{1 - 4a}{2a(1 - 2a)}\,,$$

and $(\phi, \psi)$ are elliptic coordinates defined by $\bar{X} + i\bar{Y} = k\,\cosh(\phi + i\psi)$. Here $\partial\Omega_0$ is the elliptic cylinder

$$\left(\frac{2a}{1 - 2a}\right)\bar{X}^2 + \left(\frac{1 - 2a}{2a}\right)\bar{Y}^2 = 1,$$

whose aspect ratio is given by (47). The behaviour of $\bar{\Phi}$ as $\bar{X}^2 + \bar{Y}^2 \to \infty$ provides the matching condition on the outer region that

$$w \sim ax^2 + \left(\tfrac{1}{2} - a\right)y^2 - \tfrac{1}{4}\bar{T}^2\{(\log(x^2 + y^2) - 2\log\bar{T} + 1 + \log(8a(1 - 2a))\} + O(\bar{T}^4) \tag{79}$$

as $x, y, \bar{T} \to 0$.

In the outer region $x^2 + y^2 = O(1)$, we have

$$w \sim w_e(x, y) - (t_e - t) + \pi\bar{T}^2\bar{G}(x, y) \quad \text{as} \quad t \to t_e^-,$$

where, by (79), the Green's function $\bar{G}$ must satisfy

$$\frac{\partial^2\bar{G}}{\partial x^2} + \frac{\partial^2\bar{G}}{\partial y^2} = -\delta(x)\delta(y) \quad \text{in} \quad B \quad \text{with} \quad \bar{G} = 0 \quad \text{on} \quad \partial B. \tag{80}$$

The matching also produces the result

$$t_e - t \sim -\tfrac{1}{2}\bar{T}^2\log\bar{T} + \tfrac{1}{4}\bar{T}^2\{1 + \log(8a(1 - 2a)) - 2\bar{K}\} + O(\bar{T}^4) \quad \text{as} \quad \bar{T} \to 0, \tag{81}$$

where the constant $\bar{K} > 0$ is determined by considering the local behaviour

$$\bar{G} \sim -\frac{1}{2\pi}(\log(x^2 + y^2)^{1/2} + \bar{K}) \quad \text{as} \quad x^2 + y^2 \to 0.$$

The result (48) is found by inverting (81); however, the result (81) is to be preferred because it gives $\bar{T}/(t_e - t)^{1/2}$ correct to all orders of $1/\log(1/(t_e - t))$.

We note that when $\partial B$ is a circular cylinder $x^2 + y^2 = \alpha^2$, the constant $a = \frac{1}{4}$, and the governing equations (8)-(9) can be solved exactly. The result is

$$w = \tfrac{1}{4}(x^2 + y^2) - \tfrac{1}{4}\bar{T}^2\log(x^2 + y^2) + \tfrac{1}{2}\bar{T}^2\log\bar{T} - \tfrac{1}{4}\bar{T}^2,$$

where $\bar{T}$ is given implicitly by $t = \frac{1}{4}\alpha^2 + \frac{1}{2}\bar{T}^2\log(\bar{T}/\alpha) - \frac{1}{4}\bar{T}^2$ with $t_e = \frac{1}{4}\alpha^2$.

# C 'Moments' for multiply-connected domains

## C.1 Preamble

In this appendix we derive conserved quantities for Stefan

$$\frac{1}{\beta}\frac{\partial u}{\partial t} = \nabla^2 u, \quad \text{with} \quad u = 0, \quad \boldsymbol{\nabla} u \cdot \boldsymbol{\nabla}\omega = -1 \quad \text{on} \quad t = \omega$$

and Darcy ($\beta = \infty$) moving boundary problems in which the relevant phase is multiply-connected; for the corresponding results for simply-connected domains, see King *et al.* [11] and Richardson [12], for example. We consider the class of boundary problems described above (that is, with $u = 1$ on $\partial B$ in the well-posed case, $u = -1$ in the ill-posed); the results readily generalise to other classes.

The most straightforward derivations are based on the Baiocchi transformed formulations. In the well-posed case with

$$u = u_0(\mathbf{x}) \quad \text{at} \quad t = 0 \quad \text{in} \quad B \setminus \Omega(0)$$

(here we generalise to the case in which $\Omega(0)$ does not coincide with $B$, in part to indicate how the extinction results outlined above can be extended in this fashion), we set

$$w = \int_0^t u(\mathbf{x}, t')dt' \quad \text{in} \quad B \setminus \Omega(0), \quad w = \int_\omega^t u(\mathbf{x}, t')dt' \quad \text{in} \quad \Omega(0) \setminus \Omega(t),$$

to give

$$\frac{1}{\beta}\frac{\partial w}{\partial t} = \nabla^2 w + \frac{1}{\beta}u_0(\mathbf{x}) \quad \text{in} \quad B \setminus \Omega(0), \quad \frac{1}{\beta}\frac{\partial w}{\partial t} = \nabla^2 w - 1 \quad \text{in} \quad \Omega(0) \setminus \Omega(t), \tag{82}$$

$$w = t \quad \text{on} \quad \partial B, \tag{83}$$

$$w = \frac{\partial w}{\partial n} = 0, \quad \text{on} \quad \partial\Omega, \tag{84}$$

$$w = 0 \quad \text{at} \quad t = 0 \quad \text{in} \quad B \setminus \Omega(0); \tag{85}$$

the extinction behaviour in the quasi-steady limit $\beta = \infty$ is then determined by $w_e(\mathbf{x}) = W(\mathbf{x}) + t_e$, as above, except that $W$ is now given by

$$\nabla^2 W = 0 \quad \text{in} \quad B \setminus \Omega(0), \quad \nabla^2 W = 1 \quad \text{in} \quad \Omega(0) \tag{86}$$

$$W = 0 \quad \text{on} \quad \partial B. \tag{87}$$

(In this quasi-steady limit, the function $w_e(x,y)$ is, in two dimensions, equivalent to the modified potential $\hat{\Pi}_{\Omega(0)}(x,y)$ used by Entov and Etingof [6].)

In the ill-posed case,

$$w = -\int_t^\omega u(\mathbf{x},t')dt'$$

yields, so long as a solution exists,

$$\frac{1}{\beta}\frac{\partial w}{\partial t} = \nabla^2 w - 1 \quad \text{in} \quad B\setminus\Omega(t)$$

$$w = w_0(\mathbf{x}) - t \quad \text{on} \quad \partial B,$$

$$w = \frac{\partial w}{\partial n} = 0 \quad \text{on} \quad \partial\Omega,$$

$$w = w_0(\mathbf{x}) \quad \text{at} \quad t = 0 \quad \text{in} \quad B\setminus\Omega(0),$$

where $w_0(\mathbf{x})$ is determined as described above, being underspecified if $\Omega(0)$ is empty.

## C.2 The well-posed case

Taking $\mathcal{F}(\mathbf{x})$ to satisfy

$$\nabla^2\mathcal{F} = 0 \quad \text{in} \quad B\setminus\Omega(t), \quad \mathcal{F} = 0 \quad \text{on} \quad \partial B, \tag{88}$$

an elementary calculation gives from (82)-(85) (since $u = \partial w/\partial t$)

$$\int_{B\setminus\Omega(t)} \mathcal{F}(u+\beta)\,d\mathbf{x} = \int_{B\setminus\Omega(0)} \mathcal{F}(u_0+\beta)\,d\mathbf{x} - \beta t\oint_{\partial B}\frac{\partial\mathcal{F}}{\partial n}\,dS, \tag{89}$$

or in the quasi-steady case $\beta = \infty$

$$\int_{B\setminus\Omega(t)} \mathcal{F}\,d\mathbf{x} = \int_{B\setminus\Omega(0)} \mathcal{F}\,d\mathbf{x} - t\oint_{\partial B}\frac{\partial\mathcal{F}}{\partial n}\,dS. \tag{90}$$

For $\mathcal{F}$ to be non-trivial, we require from (88) that $\mathcal{F}$ not be harmonic throughout $\Omega(t)$; for the result to apply right up to the extinction time $t_e$ we do, however, require

$$\nabla^2\mathcal{F} = 0 \quad \text{in} \quad B\setminus\{\mathbf{x}=\mathbf{x}_e\},$$

where $\mathbf{x}_e$ can be determined *a priori* in the case $\beta = \infty$, as described above. The appropriate $\mathcal{F}$ are therefore the Green's function $\mathcal{F}_0(\mathbf{x}) = G(\mathbf{x};\mathbf{x}_e)$, where $G(\mathbf{x};\boldsymbol{\xi})$ is defined by

$$\nabla^2 G = -\delta(\mathbf{x}-\boldsymbol{\xi}) \quad \text{in} \quad B, \quad G = 0 \quad \text{on} \quad \partial B, \tag{91}$$

and its derivatives of any order with respect to the components of $\boldsymbol{\xi}$, again evaluated at $\boldsymbol{\xi} = \mathbf{x}_e$,

$$\mathcal{F}_i = \left.\frac{\partial G}{\partial \xi_i}\right|_{\boldsymbol{\xi}=\mathbf{x}_e}, \quad \mathcal{F}_{ij} = \left.\frac{\partial^2 G}{\partial \xi_i \partial \xi_j}\right|_{\boldsymbol{\xi}=\mathbf{x}_e}, \ldots, \tag{92}$$

where $i, j, \ldots$ are integers between 1 and $N$; because $G(\boldsymbol{\xi}; \mathbf{x}) = G(\mathbf{x}; \boldsymbol{\xi})$ and $G$ is harmonic almost everywhere, the derivatives of second order and higher are not linearly independent. The local behaviour of these solutions at $\mathbf{x} = \mathbf{x}_e$ is given by the corresponding solutions for $B = \mathbb{R}^N$; for $N = 2$ these are proportional to

$$-\log r, \quad r^{-k}\cos(k\theta), \quad r^{-k}\sin(k\theta), \quad k = 1, 2, \ldots,$$

where $\mathbf{x} - \mathbf{x}_e = (r\cos\theta, r\sin\theta)$, and, similarly, in higher dimensions the result that if

$$\nabla^2 \phi(\mathbf{x}) = 0 \tag{93}$$

then

$$\nabla^2 \Phi(\mathbf{x}) = 0,$$

where

$$\Phi(\mathbf{x}) = |\mathbf{x} - \mathbf{x}_e|^{-(N-2)} \phi((\mathbf{x} - \mathbf{x}_e)/|\mathbf{x} - \mathbf{x}_e|^2) \tag{94}$$

enables the relevant infinite domain solutions to be expressed via (94) in terms of the solutions to (93) which are polynomials in the Cartesian coordinates (cf. King [10]).

Returning now to (89)-(90), it follows respectively that

$$\int_{B\setminus\Omega(t)} \mathcal{F}_0(u + \beta)\, d\mathbf{x} = \int_{B\setminus\Omega(0)} \mathcal{F}_0(u_0 + \beta)\, d\mathbf{x} + \beta t, \tag{95}$$

$$\int_{B\setminus\Omega(t)} \mathcal{F}_0\, d\mathbf{x} = \int_{B\setminus\Omega(0)} \mathcal{F}_0\, d\mathbf{x} + t, \tag{96}$$

while the derivatives (92) lead respectively to the conserved quantities

$$\int_{B\setminus\Omega(t)} \mathcal{F}(u + \beta)\, d\mathbf{x} = \int_{B\setminus\Omega(0)} \mathcal{F}(u_0 + \beta)\, d\mathbf{x}, \tag{97}$$

$$\int_{B\setminus\Omega(t)} \mathcal{F}\, d\mathbf{x} = \int_{B\setminus\Omega(0)} \mathcal{F}\, d\mathbf{x} \tag{98}$$

It follows from (86)-(87) that

$$W(\mathbf{x}) = -\int_{\Omega(0)} G(\mathbf{x}; \boldsymbol{\xi})\, d\boldsymbol{\xi} \tag{99}$$

and hence from (92) and $G(\boldsymbol{\xi}, \mathbf{x}) = G(\mathbf{x}; \boldsymbol{\xi})$ that

$$\frac{\partial W}{\partial x_i}(\mathbf{x}_e) = -\int_{\Omega(0)} \mathcal{F}_i(\boldsymbol{\xi})\, d\boldsymbol{\xi} \quad i = 1, 2, \ldots, N. \tag{100}$$

Moveover, setting $t = t_e$ in (98) implies that the right-hand side of (100) is zero; similarly (96) and (99) give

$$t_e = \int_{\Omega(0)} \mathcal{F}_0(\mathbf{x})\, d\mathbf{x} = -W(\mathbf{x}_e),$$

so the current approach provides an alternative but equivalent prescription of the quantities $t_e$ and $\mathbf{x}_e$ in the quasi-steady case $\beta = \infty$. More generally, the extinction time is given from (95) as

$$t_e = \int_{\Omega(0)} \mathcal{F}_0(\mathbf{x})\, d\mathbf{x} + \frac{1}{\beta}\left\{\int_B \mathcal{F}_0(\mathbf{x}) u(\mathbf{x}, t_e)\, d\mathbf{x} - \int_{B\setminus\Omega(0)} \mathcal{F}_0(\mathbf{x}) u_0(\mathbf{x})\, d\mathbf{x}\right\},$$

but this is of more limited value in the absence of information about $u(\mathbf{x}, t_e)$. For the higher derivatives in (92), one cannot simply set $t = t_e$ in (97)-(98) owing to the singular behaviour of $\mathcal{F}$ at $\mathbf{x} = \mathbf{x}_e$; we have

$$\int_{\Omega(0)} \mathcal{F}\, d\mathbf{x} = \int_B W \nabla^2 \mathcal{F}\, d\mathbf{x},$$

which gives a derivative of $W$ evaluated at $\mathbf{x} = \mathbf{x}_e$, with (97)-(98) holding only for $t < t_e$ and having discontinuous left-hand sides at $t = t_e$.

For $t > t_e$, we have $u = 1$ for all $\mathbf{x}$ when $\beta = \infty$, while for finite $\beta$ the linear diffusion problem has conserved quantities

$$\int_B e^{\lambda^2 \beta t} \hat{\mathcal{F}}_\lambda(\mathbf{x})(u(\mathbf{x}, t) - 1)\, d\mathbf{x} = \int_B e^{\lambda^2 \beta t_e} \hat{\mathcal{F}}_\lambda(\mathbf{x})(u(\mathbf{x}, t_e) - 1)\, d\mathbf{x},$$

where $\lambda$ is an eigenvalue and $\hat{\mathcal{F}}_\lambda$ the corresponding eigensolution,

$$\nabla^2 \hat{\mathcal{F}}_\lambda + \lambda^2 \hat{\mathcal{F}}_\lambda = 0 \quad \text{in} \quad B,$$

$$\hat{\mathcal{F}}_\lambda = 0 \quad \text{on} \quad \partial B.$$

## C.3 The ill-posed case

A similar derivation implies that (89)-(90), (95)-(98) remain valid, except that $t$ is replaced by $-t$ on the appropriate right-hand sides. In the case of the 'domain-filling' solutions, we require here that

$$w_0 = t_f \quad \text{on} \quad \partial B, \tag{101}$$

with the solid phase $\Omega(0)$ initially absent in which case

$$\int_{B\setminus\Omega(t)} \mathcal{F}_0(u+\beta)\, d\mathbf{x} = \beta(t_f - t),$$

with, for $t > 0$,

$$\int_{B\setminus\Omega(t)} \mathcal{F}_0(u+\beta)\, d\mathbf{x} = 0$$

for the derivatives (92). For nucleation occuring at $t = 0$, $t_f$ is determined via $\min_{\mathbf{x}\in B} w_0 = 0$. The above comments evidently apply only so long as a solution exists; the prescription for $w_0$ via (101) offers the only chance for the solution to survive until the whole domain has changed phase and, by time-reversal arguments, it will then indeed do so for $\beta = \infty$ (at least). The breakdown which will occur in other cases may simply involve the moving boundary impinging on $\partial B$, rather than developing a singularity within $B$.

# References


[1] Byrd, P. F. and Friedman, M. D. 1954 *Handbook of Elliptic Integrals for Engineers and Physicists*. Springer-Verlag, Berlin.

[2] Crank, J. 1984 *Free and Moving Boundary Problems.* Oxford University Press, New York.

[3] Chandrasekhar, S 1969 *Ellipsoidal Figures of Equilibrium* Yale University Press, New Haven.

[4] Di Benedetto, E. and Friedman, A. 1986 Bubble growth in porous media. *Indiana Uni. Math. J.* **35**, 573-606.

[5] Elliott, C. M. and Ockendon, J. R. 1982 *Weak and Variational Methods for Moving Boundary Problems.* Pitman, London.

[6] Entov, V. M. and Etingof, P. I. 1991 Bubble contraction in Hele-shaw cells. *Q. J Mech. Appl. Math.* **44**, 507-535.

[7] Friedman, A. and Sakai, M. 1986 A characterization of null quadrature domains in $\mathbb{R}^{\mathrm{N}}$. *Indiana Uni. Math. J.* **35**, 607-610.

[8] Ham, F. S. 1959 Shape-preserving solutions of the time-dependent diffusion equation. *Q. Appl. Math.* **17**, 137-145.

[9] Howison, S. D. 1986 Bubble growth in porous media and Hele-Shaw cells. *Proc. Roy. Soc. Edin.* **102A**, 141-148.

[10] King, J. R. 1991 Integral results for nonlinear diffusion equations. *J. Eng. Math.* **25**, 191-205.

[11] King, J. R., Riley, D. S. and Wallman, A. M. 1999 Two-dimensional solidification in a corner. *Proc. R. Soc. Lond.* A **455**, 3449-3470.

[12] Richardson, S. 1972 Hele-Shaw flows with a free boundary produced by the injection of fluid into a narrow channel. *J. Fluid Mech.* **56**, 609-618